Oxidation of Ethylene on Oxygen Reconstructed Silver Surfaces

Travis E Jones[1,], Regina Wyrwich[2], Sebastian Böcklein[2,†], Tulio C. R. Rocha[3], Emilia A. Carbonio[1,4], Axel Knop-Gericke[1], Robert Schlögl[1], Sebastian Günther[5], Joost Wintterlin[2], Simone Piccinin[6]*

1 Abteilung Anorganische Chemie Department, Fritz-Haber-Institut der Max-Planck-Gesellschaft, Faradayweg 4-6, 14195 Berlin (Germany). 2 Department Chemie, Ludwig-Maximilians-Universität München, Butenandtstr. 5-13, 81377 Munich (Germany). 3 Brazilian Synchrotron Light Laboratory, Caixa Postal 6192, CEP 13083-970, Campinas (Brazil). 4 Helmholtz-Zentrum Berlin für Materialien und Energie GmbH, BESSY II, Albert-Einstein-Str. 15, 12489 Berlin (Germany). 5 Chemie Department, Technische Universität München, Lichtenbergstr. 4, 85748 Garching (Germany). 6 CNR-IOM DEMOCRITOS, Consiglio Nazionale delle Ricerche- Instituto Officina dei Materiali c/o SISSA, Via Bonomea 267, 34136 Trieste (Italy).

†Current Address: Clariant Produkte (Deutschland) GmbH, Waldheimer Str. 13, 83052 Bruckmühl (Germany)

1

Abstract

We report on theoretical and experimental studies of the reactivity of ethylene with oxygen in two well-known oxygen induced surface reconstructions on silver, the p(2x1) reconstruction on the Ag(110) and the p(4x4) reconstruction on the Ag(111) surfaces. Density functional theory calculations demonstrate that ethylene can react with oxygen on both surfaces to form an oxametallacycle that can decompose into either ethylene oxide or a CO_2 precursor, acetaldehyde. The activation energy associated with acetaldehyde formation is predicted to be 0.4 eV lower than that associated with epoxide formation on both surfaces, though we find lower barriers for all elementary steps on the p(4x4) reconstruction due to its unique structural dynamics. Our calculations predict these dynamics make the p(4x4) reconstruction active in acetaldehyde formation at room temperature. Experiments performed by exposing the p(4x4) reconstruction to ethylene at room temperature support this finding with CO_2 the only carbonaceous product formed during temperature programed desorption. Our results unambiguously demonstrate that, alone, these oxygen reconstructions are not selective in ethylene epoxidation on silver.

Introduction

The unique ability of silver to catalyze the partial oxidation of ethylene to ethylene oxide in O_2 has long been of interest to the chemistry community and is the subject of numerous reviews [1-4]. In this apparently simple reaction a single oxygen atom is added to ethylene to yield ethylene epoxide. The challenge and interest arises from the fact that ethylene oxide is not the thermodynamically favored product under an oxidizing atmosphere, CO_2 is. Yet, unpromoted silver has the ability to produce the epoxide with nearly 50% selectivity, a value that can be

increased to over 90% with the addition of promoters and inhibitors [1-5]. Identifying the origin of this behavior under realistic conditions is one of the most fundamental challenges in heterogeneous catalysis.

There is widespread agreement that ethylene epoxidation occurs through a Langmuir–Hinshelwood mechanism [6], with the notable exception of ethylene epoxidation on Ag_2O, where computational studies suggest EO is produced through an Eley-Rideal type mechanism if no $Ag^{\delta+}$ surface sites are available for ethylene adsorption [7, 8]. However, there is no consensus on the nature of the species active in epoxidation and combustion [6]. Thermodynamic considerations are often used to rule out the involvement of Ag_2O, as the bulk oxide is not stable under epoxidation conditions [11-6, 9]. Instead, at the oxygen chemical potentials required for epoxidation surface reconstructions with $Ag^{\delta+}$ sites available for ethylene adsorption are formed [6, 10, 11]. Such structures have been observed directly by scanning tunneling microscopy (STM) [10, 11] and the presence of chemically similar oxygen species under near ambient pressure conditions can also be inferred by *in situ* X-ray photoelectron and near edge X-ray absorption spectroscopies (XPS and NEXAFS) [12-15]. (Note that in the earlier publications the p(4x4) phase on Ag(111), which has played a central role in the discussion, was considered a 2D oxide-like structure but in 2006/2007 was shown to be a reconstruction [16-18].) Such results have similarly been predicted by *ab initio* calculations suggesting that silver surfaces are covered with oxygen-induced surface reconstructions at the oxygen chemical potentials typical for epoxidation under industrial conditions, while a low coverage of oxygen adatoms on an unreconstructed Ag surface is only stable at lower oxygen chemical potentials [9, 15]. However, due to the long-standing difficulty associated with resolving the structure of some of these

surface reconstructions [16-19], we know of no complete theoretical study of their behavior in epoxidation. Thus, their role remains unclear.

One common hypothesis is that the surface reconstructions serve to produce $Ag^{\delta+}$ sites for ethene adsorption and that the partially ionic oxygen involved in the reconstructions can only participate in total oxidation [20]. Titration of the oxygen induced p(2x1) reconstruction on an Ag(110) single crystal with ethylene appears to confirm this view, as only CO_2 is produced in such experiments [21]. However, a second hypothesis is that oxygen in these surface reconstructions can be incorporated in ethylene oxide [22]. In support of this view, temperature programmed reduction of supported silver catalysts yields epoxide with near 50% selectivity [23], where the active species was argued to be consistent with the high coverage of oxygen on the Ag(111) surface typical in, for example, the p(4x4) reconstruction [16-19].

Contrast this state of knowledge to that of adsorbed atomic oxygen on unreconstructed Ag surfaces. Experimentally, STM measurements performed at 4 K reveal that such a state might be present when the oxygen coverage is below 0.05 ML [24], above which coverage reconstructions nucleate [24]. However, low-energy electron microscopy (LEEM) experiments performed at ~500 K are unable to confirm the presence of this low-coverage phase of partially-ionic unreconstructed atomic oxygen [25, 26] and establish an upper limit of 0.03 ML for such a phase [26]. Despite this discrepancy, numerous density functional theory (DFT) calculations have been performed on the mechanism of ethylene epoxidation on silver with adsorbed atomic oxygen on unreconstructed Ag surfaces. These have revealed, in agreement with kinetic isotope studies [27], that epoxidation and combustion can proceed through a common intermediate [28-33]. Within this mechanism the common intermediate, an adsorbed oxametallacycle (OMC), can isomerize to EO or acetaldehyde (AcH), which rapidly burns [34, 35]. Because the two

isomerization pathways are associated with competing elementary steps, the difference between the activation energies of them is often viewed as providing a computationally accessible upper limit of EO selectivity. However, because the two activation energies are often quite similar the predicted selectivity is near 50% for all surfaces, oxygen coverages, and binding sites [32], while experimentally selectivity is sensitive to materials, conditions, and sample history [1-6, 12, 14]. Furthermore, there is scarce evidence that a measurable amount of the more ionic type of oxygen modeled by DFT is present under epoxidation conditions [15, 36] because it forms surface reconstructions at oxygen chemical potentials relevant for ethylene epoxidation [10, 19, 21].

   Herein we investigate the behavior of two well-known and well-characterized oxygen reconstructed silver surfaces, the p(4x4) structure on the Ag(111) surface and the p(2x1) structure on the Ag(110) surface, with ethylene in an effort to identify the role of these types of surfaces in ethylene epoxidation. Through a combination of calculated minimum energy paths and surface science experiments we conclude that the $Ag^{\delta+}$ sites in the reconstructions can adsorb ethylene, but that the oxygen in these surface reconstructions can only participate in total combustion. This observation supports the idea that a second species [5, 12, 14, 20, 25], often referred to as *electrophilic oxygen*, is required for ethylene epoxidation.

Theoretical and Experimental Methods

   DFT calculations were performed with the Quantum ESPRESSO package [37] using the Perdew, Burke, and Ernzerhof (PBE) exchange and correlation [38]. We used ultrasoft pseudopotentials taken from the PS library [39] with a kinetic energy (charge density) cutoff of 30 Ry (300 Ry) and Marzari-Vanderbilt cold smearing [40] with a smearing parameter of 0.02 Ry. Increasing these cutoffs resulted only in minor changes to the computed activation energies,

see Table S1. We also tested the role of adding a van der Waals correction using both Grimme's approach [41] and the exchange-hole dipole moment (XDM) dispersion model [42, 43], see Table S2. We find that this contribution leads to changes in activation energies of around 0.1 eV, a value small enough to ensure that none of the conclusions presented here are affected. It does not change the picture presented here and will not be discussed further. Five-layer silver slabs were used with the computed lattice constant (4.15 Å) and a Monkhorst-Pack **k**-point mesh equivalent to (12x12) for the (1x1) surface unit cell. A p(4x4) cell was employed for the Ag(111) and a p(2x2) cell for the Ag(110) reconstruction. The minimum energy paths were computed using the climbing image nudged elastic band (NEB) method with the bottom two layers of the slabs held fixed. Each path was discretized into 8 images with a single transition state separating local minima. We considered the transition states to be converged when the force on the climbing images was less than 0.05 eV/Å and the change in energy simultaneously was less than 10^{-3} eV. We ensured the NEB calculations converged to the transition states through normal mode analyses. Core level binding energies were computed using the ΔSCF procedure to capture initial and final state effects [38]. The relative values computed in this way were shifted to absolute values using a reference state calculation on a (2x2x2) cell of Ag_2CO_3 and the corresponding measured binding energies [39]. We have previously found this approach to give computed binding energies to within ±0.3 eV of experimental values [15]. For a full description of our approach see Reference [15].

We tested the theoretical predictions for the p(4x4) reconstruction through temperature programmed reaction (TPR). The experiments were carried out in a combined ultra-high vacuum (UHV)/ambient pressure system described in detail elsewhere [46]. The sample was cleaned by multiple cycles of Ar^+ sputtering and subsequent heating to 775 K. To avoid high oxygen doses

the clean Ag(111) surface was dosed with ~600 L NO_2 at 500 K to produce the p(4x4) reconstruction following an established procedure [47]. We know from LEED performed after earlier experiments that this procedure leads to the formation of the oxygen induced p(4x4) reconstruction, which we verified by an XPS O 1s binding energy (BE) of 528.3 eV. XPS measurements were carried out with a monochromatic Al Kα source (Omicron XM 1000) and a hemispherical analyzer (SPECS Phoibos 100). The energy axis of the spectra was calibrated using the Ag $3d_{5/2}$ peak with a BE of 368.25 eV. After preparation of the p(4x4) reconstruction the sample was dosed with 54000 L C_2H_4 at room temperature and investigated with TPR and XPS. In a second set of experiments ethylene was dosed at 0.1 mbar for 10 min at 298 K. For the TPR experiment, the sample was heated at 0.8 K/s. Products were measured by a quadrupole mass spectrometer (Pfeiffer Prisma QMS 200 M2).

Results

Ethylene oxidation on the p(2x1)-reconstructed Ag(110) surface

Atomically adsorbed oxygen on the Ag(110) is populated with a sticking coefficient of approximately 2×10^{-3} at room temperature, giving rise to a p(Nx1), so-called added-row reconstruction, where N ranges from 2-7 [48]. At 423 K this relatively high sticking probability allows the p(2x1) reconstruction to be formed at pressures as low at 10^{-4} mbar [12]. Furthermore, this reconstruction is known to be present on Ag(110) single crystals after ethylene epoxidation at ~500 K with O_2 pressures from 5-200 mbar [21]. The ease with which the p(2x1) reconstruction can be prepared has allowed it to be thoroughly characterized [15, 49, 50]. This fact, along with its ubiquity, makes the p(2x1) added-row reconstruction a good system with which to begin our current study.

The name, added-row, stems from the formation mechanism according to which adsorbed O and Ag atoms condense on the terraces to form Ag-O chains along the [001] directions of the surface with (2x1) periodicity [51], as shown in Figure 1. This bonding topology is reminiscent of the linear Ag-O bonding in the bulk oxide, Ag_2O, [15] and leads to the formation of $Ag^{\delta+}$ in the added rows, as evidenced by their computed Ag3d shift (including final state effects) of -0.4 eV with respect to bulk silver. The charge transfer to oxygen also leads to a measured/computed oxygen O 1s binding energy of approximately 528.3 eV, which is less than that seen in bulk Ag_2O (529.2 eV) [15], indicating that the Ag-O bonding is partially ionic in this system.

Computationally we find that ethylene adsorbs on the $Ag^{\delta+}$ site in the added rows, which is the first step in the oxidation path shown in Figure 1. Ethylene adsorption on the $Ag^{\delta+}$ site, labeled (1) in Figure 1, is associated with 0.11 eV drop in energy. (For convenience the energies along the minimum energy paths are collected in Table 1.) Consistent with this low heat of adsorption is a negligible increase in a C-C bond length, from 1.33 Å in the gas phase to 1.34 Å when adsorbed, in agreement previous NEXAFS measurements that indicated ethylene adsorbs by transferring π density to $Ag^{\delta+}$ [52].

In the second elementary step of Figure 1 adsorbed ethylene reacts with an oxygen atom from the added row to form an OMC producing state (2) in the figure. The activation energy associated with this step is 0.44 eV, and the formation of the OMC is accompanied by a 0.17 eV drop in energy with respect to the adsorbed ethylene. Inspection of the figure reveals that the OMC is highly twisted, thereby allowing the linear Ag-O bonding motif of the added rows to be maintained. This twisting can be seen to result in a staggered conformation for the hydrogen atoms in the OMC, with an O-C-C-Ag dihedral angle of 76°. There is also a reduction in C-C bond order, resulting in the elongation of the C-C bond to 1.51 Å.
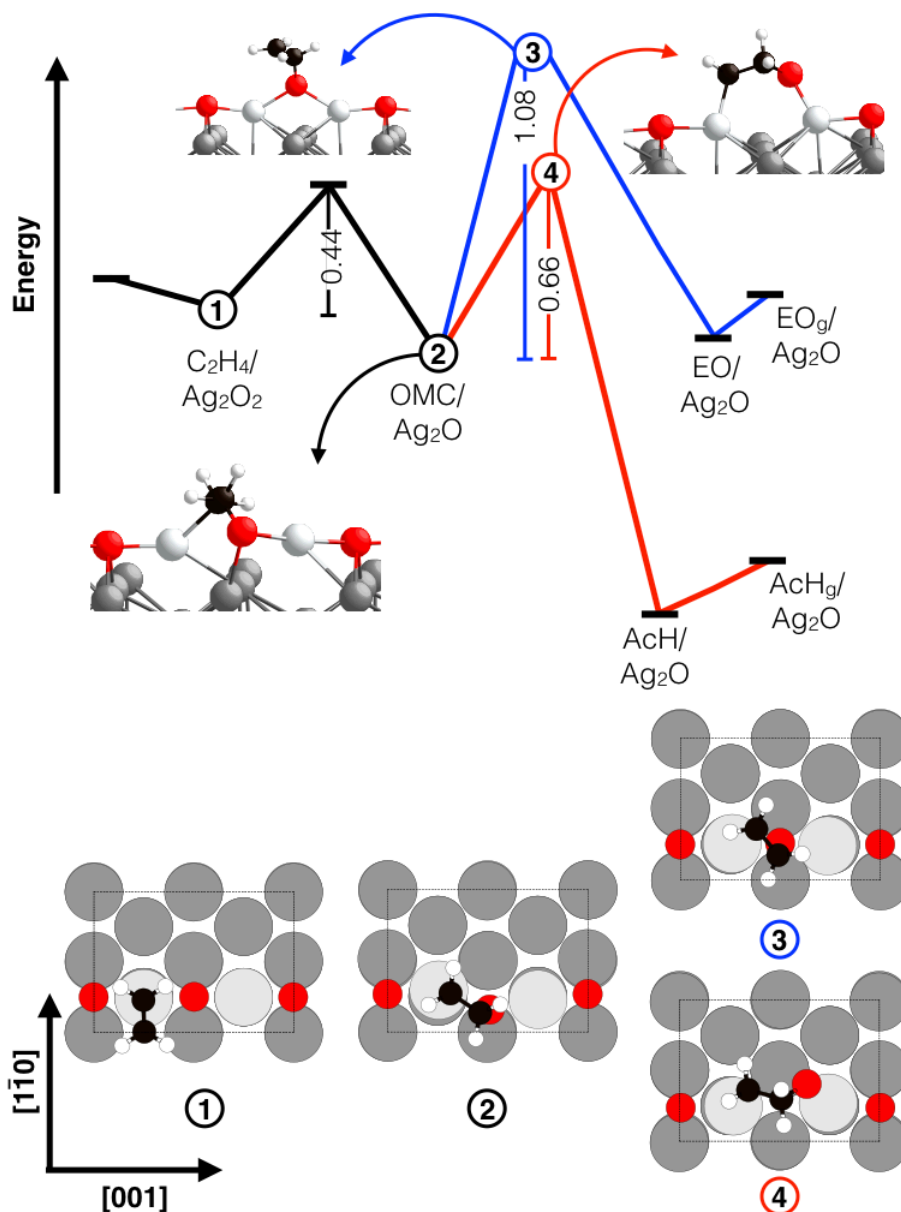
Figure 1: The minimum energy path computed for reaction of ethylene with oxygen in the p(2x1) reconstruction on the Ag(110) surface through the OMC mechanism. The silver in the added row are light gray, the underlying silver are dark gray, oxygen are red, carbon are black, and hydrogen are white. Structure (1) shows the adsorbed ethylene, (2) the OMC intermediate, (3) the transition state leading to EO, and (4) the transition state leading to AcH. The activation energies for the elementary steps are given in eV. See Table 1 for other energies.

Table 1: Computed adsorption energies (E_{ads}), with respect to gas phase C_2H_4 and the unmodified surface reconstructions, of the partial oxidation intermediates on the reconstructed Ag(110) and Ag(111) surfaces along with their corresponding activation energies (E_a). The formation energy (E_f) of the products is also shown with the same energy reference. The two sets of energies for AcH formation for the Ag(111) surface refer to the two pathways discussed in the text. The states corresponding to the labels in Figures 1 and 3 are also listed. All values are reported in eV.

system	$E_{ads}(C_2H_4)$ State 1	E_a(OMC)	E_{ads}(OMC) State 2	E_a(EO) State 3	E_f(EO)	E_a(AcH) State 5 (4)	E_f(AcH)
Ag(110)-p(2x1)	-0.11	0.44	-0.28	1.08	-0.35	0.66	-1.31
Ag(111)-p(4x4)	-0.08	0.38	-0.03	0.66	-0.16	0.29 (0.71)	-1.30 (-1.29)

Once the OMC has formed it can isomerize to EO and AcH, as has been calculated for ethylene epoxidation with adsorbed atomic oxygen on the unreconstructed surface [28-33]. However, unlike adsorbed atomic oxygen on the unreconstructed surface, where the EO and AcH activation energies are nearly equal, the barrier to EO formation is significantly higher than that associated with AcH formation on this reconstructed Ag(110) surface, 1.08 eV and 0.66 eV, respectively. This can be rationalized by the fact that the hydrogen atoms in the OMC have a staggered geometry, which facilitates the hydrogen shift from C_1 (carbon bound to O in the OMC) to C_2 (carbon not bound to O in the OMC) [53]. Thus, assuming similar pre-factors for the two competing rearmaments, our calculations predict that, with an EO selectivity on the order of

10^{-4} at 500 K, the oxygen-induced p(2x1) reconstruction on the Ag(110) surface will produce only AcH through the OMC mechanism. However, the aldehyde is not the terminal product on this surface. Instead, AcH has been shown to rapidly convert into acetate on an oxygen-covered Ag(110) surface [54], which, under epoxidation conditions, further reacts with adsorbed oxygen to produce CO_2 [55]. The finding that the oxygen-induced p(2x1) reconstruction is incapable of producing EO is in agreement with previous experimental work [21].

Ethylene oxidation on the p(4x4) reconstruction of Ag(111)

Though the finding that the oxygen-induced p(2x1) reconstruction on silver strongly favors AcH production through an OMC mechanism, and ultimately combustion, is interesting, the analysis of temperature programed desorption (TPD) data suggests much of the oxygen on high surface area catalysts is adsorbed on close-packed faces [23]. And while the oxygen-induced reconstructions on the Ag(110) surface appear oxidic due to their linear Ag-O-Ag bonding motif, the oxygen-induced reconstructions on the Ag(111) surface are unlike any known bulk phases [16-19]. This novel bonding may also lead to unique chemistry.

The p(4x4) oxygen-induced reconstruction is the prototype and most well-studied member [16-18] of a family of similar surface reconstructions on the Ag(111) surface [19]. This structure is now known to be comprised of two Ag_6 triangles in the (4x4) cell with a pair of oxygen atoms shared between each Ag_6 edge as shown in Figure 2 [15-19]. In our 0 K DFT calculations one of the oxygen atoms in each pair sits 0.55 Å above the Ag_6 triangles while the other member of the pair is 0.24 Å below the triangles. This difference in oxygen atom height leads to the azimuthal rotation of the Ag_6 triangles indicated by way of the curled arrows in Figure 2. The corners of neighboring triangles are separated by 3.06 Å, atoms labeled 1 and 2, when the shared oxygen

atom is above the Ag_6 plane and is 3.76 Å, atoms labeled 3 and 4, when the oxygen sits below the Ag_6 plane. However, this clockwise and counterclockwise rotation of the silver triangles is thought to change dynamically already at room temperatures [16].
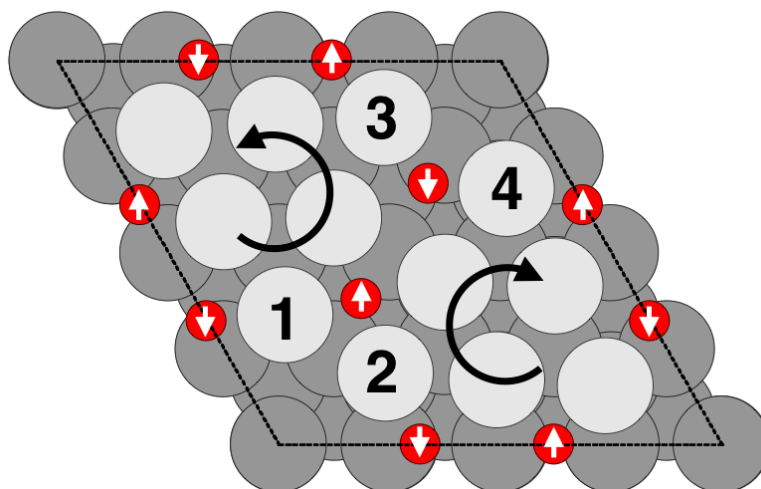

Figure 2: The p(4x4) oxygen-induced reconstruction of the Ag(111) surface. The black arrows indicate the azimuthal rotation of the Ag_6 triangles. The oxygen atoms are colored red, the silver atoms in the Ag_6 triangles are light gray, and the underlying silver is colored dark gray. The white arrows on the oxygen atoms indicate whether they lie above (up arrows) or below (down arrows) the plane of the Ag_6 triangles.

Despite the p(4x4) reconstruction's dissimilarity to the bulk oxide, Ag_2O, the Ag-O bonding also leads to the formation $Ag^{\delta+}$ in the silver triangles, as indicated by a Ag 3d shift of between -0.3 eV and -0.6 eV relative to the bulk metal [56]. And, as with the $Ag^{\delta+}$ in the oxygen-induced reconstruction on the (110) surface, on the (111) surface this positive charge on Ag facilitates ethylene adsorption. The computed favored adsorption site, see Figure 3 state (1), agrees with previous STM measurements [11], though it should be noted that these measurements were originally interpreted with a since disproven 2D oxide-like model of the p(4x4) structure. While

our computed adsorption site on the Ag_6 triangle is in agreement with previous experiments, the interaction with the correct model of the p(4x4) reconstruction is weaker than what was predicted on the early oxide-like model [11]. In our case ethylene adsorption on the favored $Ag^{\delta+}$ site is 0.08 eV exothermic and is accompanied by a lengthening of the C-C bond to 1.34 Å, similar to the oxygen-reconstructed Ag(110) surface previously discussed. Again, the energies along the minimum energy paths are summarized in Table 1. For comparison, the adsorption energy on the disproven oxide-like model of the p(4x4) reconstruction was previously computed to be 0.39 eV and the C-C bond length 1.37 Å. We did not consider this model in our calculations and refer the interested reader to Reference [11].

We find that, once adsorbed, the ethylene can react with the oxygen lying above the plane to form an OMC by surmounting a barrier of only 0.38 eV. This elementary step is weakly endothermic, raising the energy of the system by 0.05 eV with respect to the adsorbed ethylene. (Note that reaction with the oxygen below the plane increases the energy of the system a further 0.29 eV and will not be considered further.) The resultant intermediate, and its position along the reaction path, is shown in Figure 3 state (2). A more detailed view of the OMC is shown in Figure 4. As on the Ag(110) surface, the C-C bond in the OMC is stretched to 1.50 Å. However, unlike on the Ag(110) surface, the OMC on the p(4x4)/Ag(111) surface is characterized by nearly eclipsed hydrogen atoms. The two symmetry unique pairs of cis-hydrogen atoms have H-C-C-H dihedral angles of 1° and 12°, see Figure 4. For simplicity we will refer to these as the 1°-eclipsed and 12°-staggered hydrogen atoms, respectively.
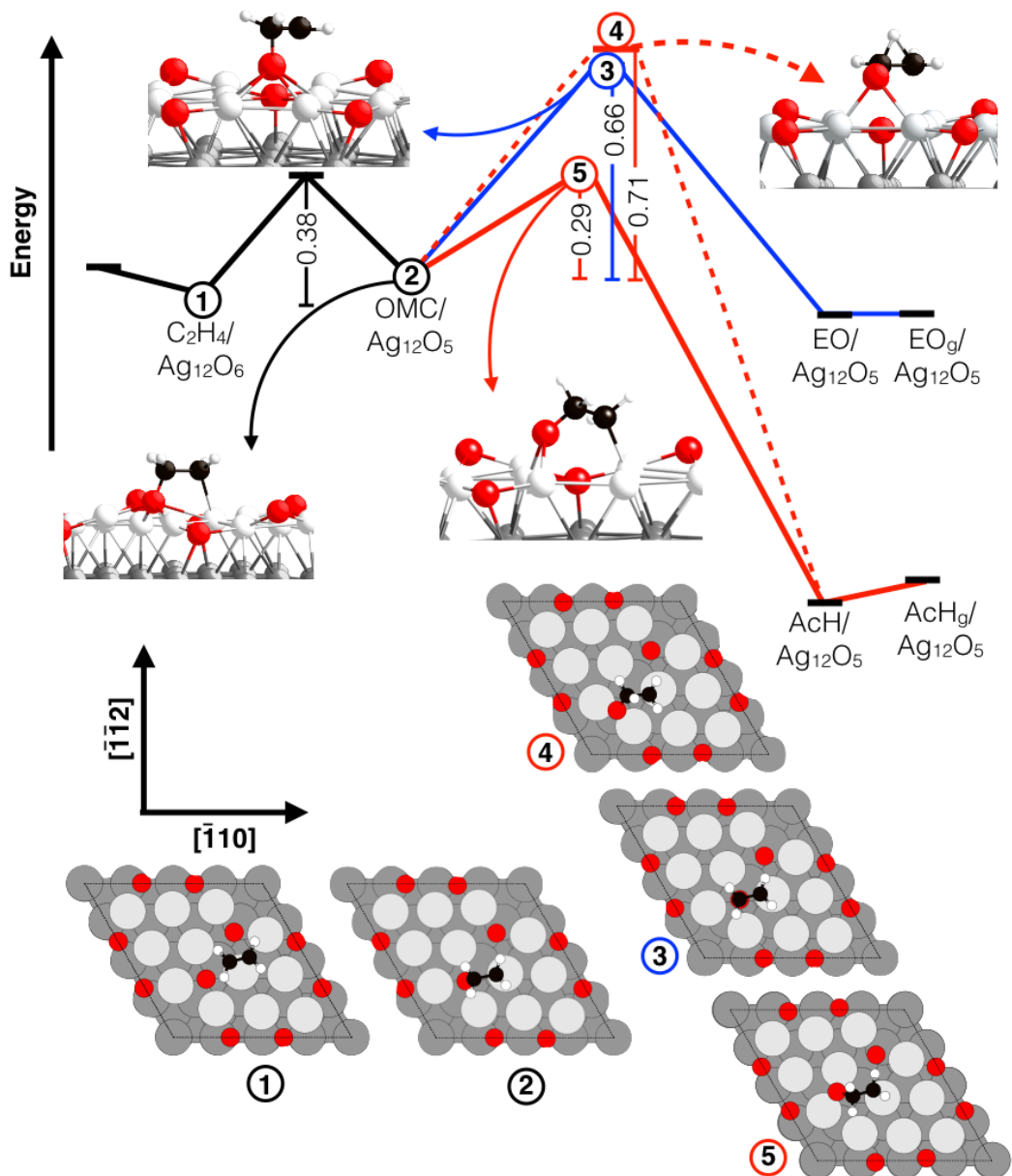
Figure 3: Minimum energy paths for AcH and EO formation on the p(4x4) oxygen induced reconstructed Ag(111) surface through the OMC mechanism. The oxygen atoms are colored red, the silver atoms in the Ag_6 triangles are light gray, the underlying silver is colored dark gray, carbon atoms are black, and oxygen atoms are white. State (1) shows the adsorbed ethylene, (2) the OMC, (3) the transition state to EO, (4) the transition state to AcH associated with the

14

eclipsed hydrogen, (5) the transition state to AcH associated with the staggered hydrogen. The activation energies for the elementary steps are given in eV. See Table 1 for other energies.
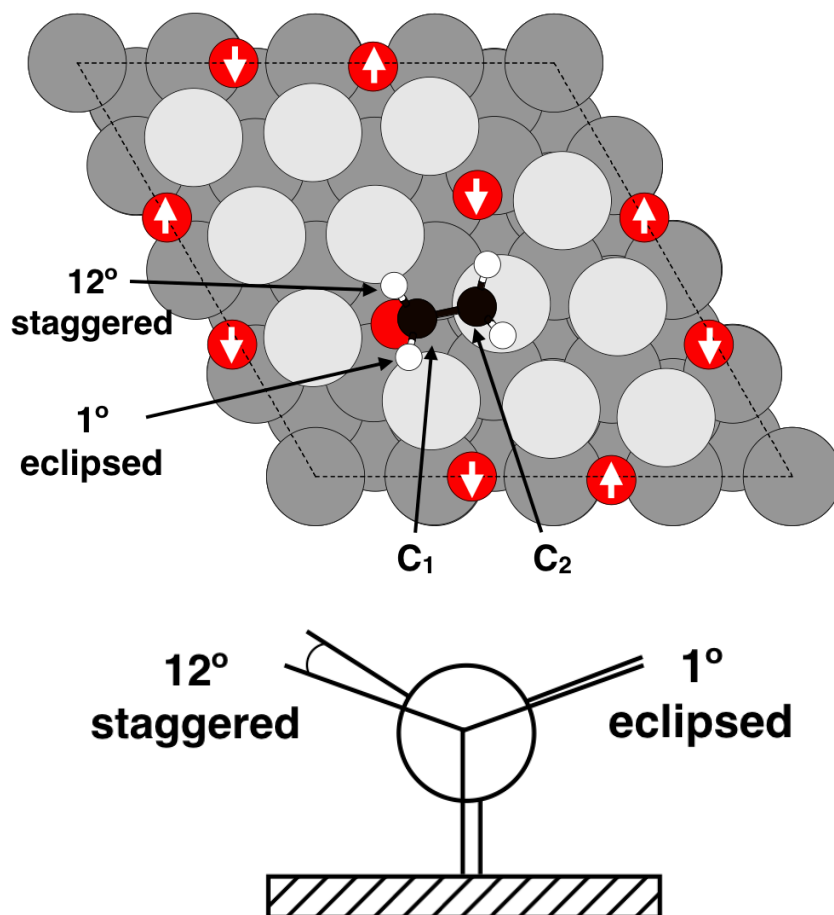

Figure 4: Ball and stick model of the OMC on the p(4x4) reconstruction on the Ag(111) surface [the same as state (2) in Figure 3] with the two types of hydrogen and carbon atoms labeled (top). The coloring is identical to Figure 3. Arrows have also been placed on the oxygen atoms to denote whether they lie above (up arrow) or below (down arrow) the plane of the Ag_6 triangles. The oxygen in the OMC lies above the Ag_6 triangles. Schematic of the OMC confirmation viewed along the C-C bond axis (bottom).

From the results on the (110) surface, and those presented in Ref. [53], we might expect the AcH/EO branching ratio to favor EO on the (111) surface when the shift of a hydrogen atom from C_1 (near the O atom, see Figure 4) to C_2 (see Figure 4) involves the 1°-eclipsed hydrogen in the OMC on the p(4x4)/Ag(111) surface. Comparing states (3) and (4) in Figure 3 reveals this is the case. The figure shows the sole minimum energy path we find for ring closure and EO formation through state (3), with a barrier of 0.66 eV and a -0.13 eV heat of reaction for the elementary step. The transition state for the C_1 to C_2 shift of the 1°-eclipsed hydrogen atom, shown in state (4), is marginally higher, at 0.71 eV. This elementary step for AcH formation is 1.26 eV exothermic with respect to the OMC. Here, as with the Ag(110) surface, the difference in activation energies can be rationalized by the OMC's propensity towards the C_1 to C_2 hydrogen shift. However, the reconstructed Ag(111) surfaces differ from their Ag(110) counterparts in that the former have been argued to be dynamic, with the Ag_6 triangles thought to rotate between equivalent positions, as indicated in Figure 2 [17]. We find that this dynamic behavior imparts an unexpected chemistry when examining the C_1 to C_2 shift of the 12°-staggered hydrogen.

State (5) in Figure 3, which is reproduced in Figure 5 for clarity, shows the transition state for the C_1 to C_2 shift of the 12°-staggered hydrogen atom in the OMC. The activation energy for this elementary step is only 0.29 eV, significantly less than that observed for other OMC decomposition pathways on silver [33]. We find that the barrier is reduced by the dynamics of the reconstruction. At the transition state these dynamics allow the Ag_6 triangle labeled with an arrow in Figure 5 to rotate ~3° counterclockwise with respect to its initial position [state (2) in Figure 3]. This rotation leads to a reduction in the Ag-Ag distance of the atoms labeled 1 and 2 in

Figure 5 from 3.32 Å in the OMC [state (2) in Figure 3] to 2.86 Å, slightly less than the DFT-calculated Ag bulk interatomic distance of 2.94 Å.

The Ag_6 triangle rotation and the Ag-Ag bond formation significantly reduce the energy at the transition state. To quantify this reduction we performed a NEB calculation wherein only the C, H, and O atoms of the OMC were allowed to relax during AcH formation. The remaining Ag and O atoms were linearly transformed from their initial to final state positions along the NEB path. Suppressing the substrate rotation in this way increased the activation energy to 0.88 eV compared to 0.29 eV for the dynamic surface. Thus, if similar pre-factors for AcH and EO isomerization are assumed, the dynamic nature of the p(4x4) structure makes it selectively produce AcH, with an EO selectivity on the order of 10^{-4} at 500 K. However, as on the (110) surface, AcH is not expected to be the terminal product on the p(4x4) reconstruction [57, 58].

Although we made no attempt to compute the mechanism of the rapid combustion chemistry of AcH on the p(4x4) reconstruction, from previous high resolution reflection absorption infrared spectroscopy (RAIRS) studies we know that at saturation coverage this AcH will be completely converted into adsorbed acetate by 220 K under UHV and to CO_2 by 450 K [57]. By analogy with the (110) surface it appears plausible that, at lower coverage, acetate may also react with adsorbed oxygen to produce formate at temperatures significantly (~200 K) less than the UHV decomposition temperature of acetate [55]. Formate, however, also decomposes to form CO_2, albeit at 350 K [58], indicating that regardless of the exact pathway the terminal product for AcH under epoxidation conditions on this surface is CO_2. Thus, as with the p(2x1) reconstruction on the Ag(110) surface, we expect the p(4x4) reconstruction on the Ag(111) surface to selectively produce CO_2.
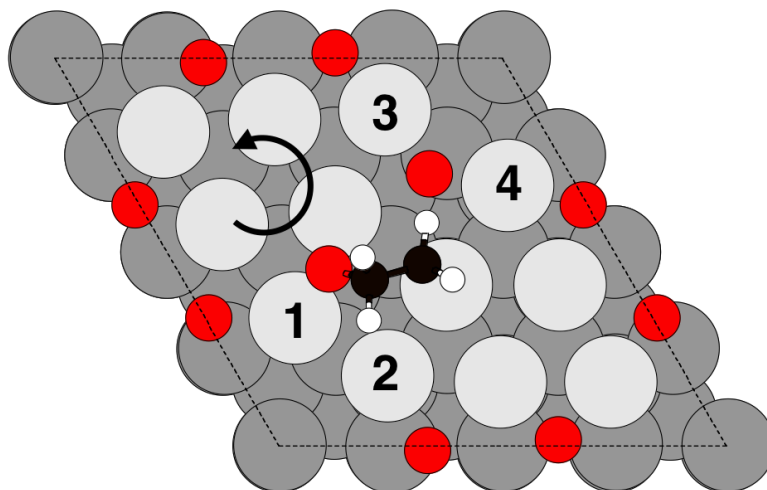
Figure 5: Transition state for the barrier pathway to AcH on the p(4x4) reconstruction on the Ag(111) surface through the C_1 to C_2 shift of the 12°-staggered hydrogen. The coloring is identical to Figure 3. The rotation of the surface Ag_6 triangle is indicated by an arrow. An enlarged side view of this structure is given in the supporting information.

The computational prediction that neither surface reconstruction can produce EO through the OMC mechanism may come as a surprise considering that the p(4x4) reconstruction has often been viewed as a prototypical active surface oxide [16] and there is spectroscopic evidence that this type of oxygen is present under reaction conditions [12, 15]. To validate our theoretical predictions we performed a series of TPR experiments on an Ag(111) single crystal.

After preparing the single crystal with NO_2 we verified that the p(4x4) reconstruction was present by XPS (see Figure 6). There were also traces of re-adsorbed NO/NO_2 present, as can be seen by the small peak at 531.65 eV, characterizing NO on the O-covered surface [59]. We then dosed ethylene at room temperature. At this temperature we predict from our DFT results that the ethylene will adsorb on the $Ag^{\delta+}$ sites, as in state (1) of Figure 3, and surmount the small (0.29

eV) barrier to form AcH. The aldehyde is then expected to rapidly convert into acetate [57] or formate [58] and eventually CO_2 near room temperature [57, 58].
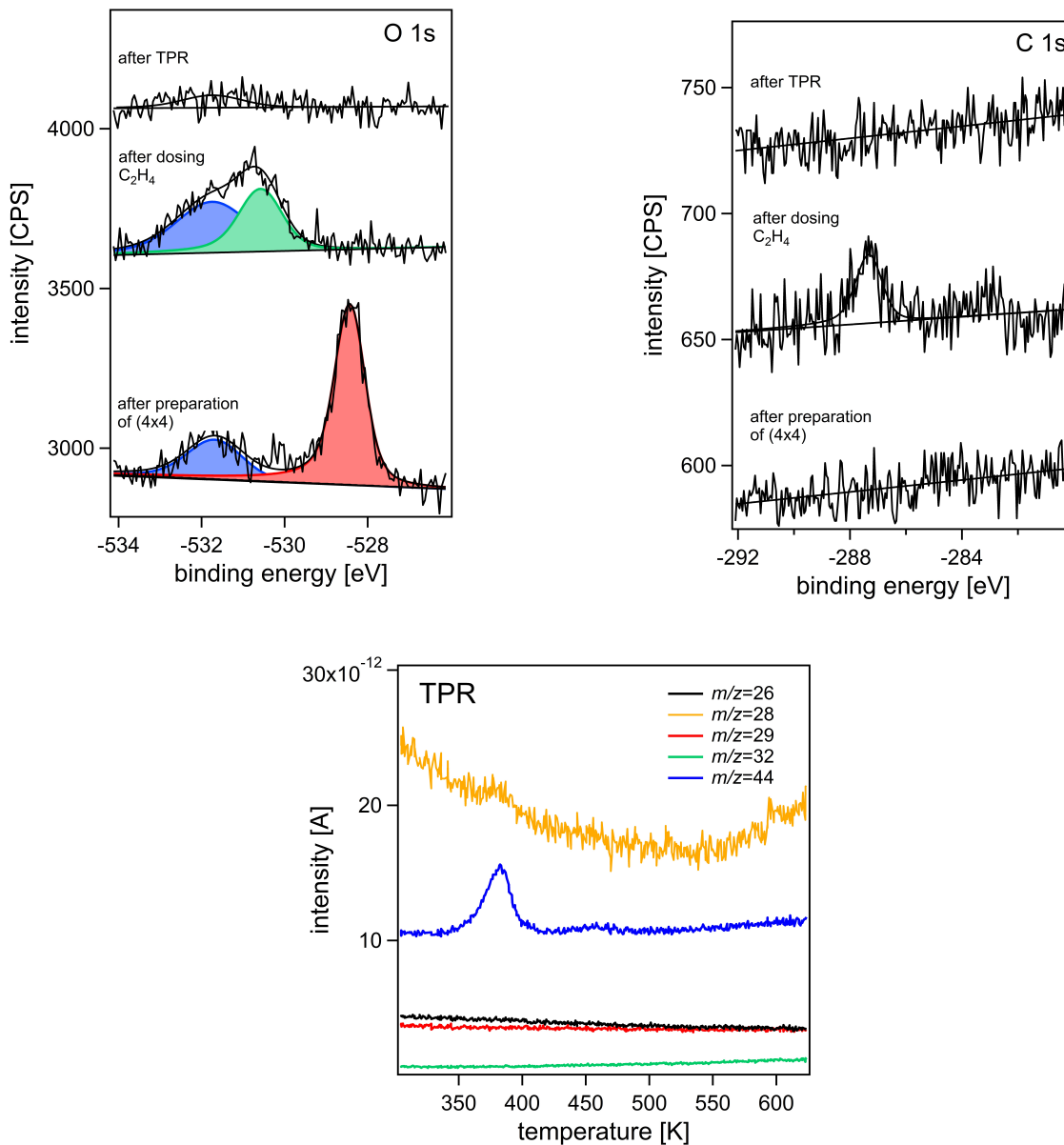

Figure 6: O 1s spectra (left) of the as prepared p(4x4) reconstruction, the surface after ethylene dosing, and the Ag(111) surface after the TPR experiment. The corresponding C 1s spectra are also shown (right). The small peak in the C 1s spectrum at 283 eV after ethylene dosing indicates the presence of some additional form of reduced carbon. For better visibility the spectra were

displaced on the intensity axis. QMS signals obtained during the TPR experiment (bottom). The noise of the $m/z = 28$ trace comes from the subtraction of a high background signal.

In support of this assertion, the XP spectra after dosing C_2H_4 shows that the p(4x4) reconstruction has vanished and that a new peak appears. This peak can be deconvoluted into two peaks, indicating the presence of two species, readsorbed NO/NO_2 at 531.65 eV and a second species at 530.5 eV. Inspection of the C 1s spectrum reveals an oxidized carbon species with a BE 287.3 eV suggesting the oxygen species with an O 1s BE of 530.5 eV is bound to carbon. Our core level BE calculations (see Table 2) reveal that formate and acetate are the most likely of the plausible $H_xC_yO_z$ species that could give rise to these C 1s and O 1s features, with formate giving the best agreement with both the C 1s and O 1s energies. Though the statistics of the carbon spectra are quite poor because of the low cross-section of the C 1s signal with Al Kα irradiation (0.013 for C 1s, 0.04 for O 1s) [60], the cross section-corrected ratio (O 1s 530.5 eV/C 1s 287.3 eV) is 2.5, implying that primarily a H_xCO_2 species like formate is present after ethylene dosing. Such a formate species is expected to decompose into CO_2 at ~350 K [58]. Thus, in a second experiment we heated the likewise prepared sample at 0.8 K/s directly after ethylene dosing to desorb the products that were monitored by QMS.

Table 2: Computed core level binding energies of oxidized carbon species on the p(4x4) reconstruction on the Ag(111) surface. All values are in eV and were computed using the ΔSCF method to include both initial and final state effects. In cases where there are multiple atoms of the same type all respective core level binding energies are listed.

System	O 1s [eV]	C 1s [eV]
C_2H_4	--	284.8, 284.8
OMC	529.9	285.8, 283.2
OH	530.5	--
AcH	531.2	286.5, 286.2
Acetate	530.8, 530.7	287.7, 285.8
Formate	530.9, 530.9	287.5
CO_2	534.1, 534.1	289.6
Measured	531.6, 530.5	287.3

Typically in this type of TPR experiment the presence of EO is determined by the mass fragment $m/z = 29$ amu. However, owing to the challenges associated with discerning partial oxidation products from the natural 2.2% $^{12}C^{13}CH_4$ isotope in ethylene using $m/z = 29$ amu on the Ag(111) surface [61], we monitored both $m/z = 29$ amu and $m/z = 26$ amu. Doing so allows us to rule out the possibility of ethylene desorption as a source of $m/z = 29$ amu. We also monitored the CO_2 mass $m/z = 44$ amu, which has cross sensitivity with the primary EO mass, but, as we have a secondary means of EO detection, this cross sensitivity is not problematic. Finally, to see if any oxygen remains unreacted we measured $m/z = 32$ amu.

The QMS results from the TPR experiment are shown in Figure 6. We saw that $m/z = 44$ amu and $m/z = 28$ amu show a maximum at approximately 380 K, somewhat higher than the 350 K measured for formate decomposition on this surface [58]. The intensities are in accordance with the fragmentation pattern of CO_2 [61]. In addition, the $m/z = 44$ amu showed a very small peak at about 460 K, which is close to the 450 K previously measured for acetate decomposition on this surface [57], indicating that some acetate may have been present. We interpret these results as the decomposition of formate and acetate and subsequent desorption of CO_2. We were, however, unable to detect concomitant desorption of H_2 or H_2O.

The measured desorption temperatures of $m/z = 44$ amu are in line with those seen during similar TPR experiments on high surface area catalysts [23]. However, unlike results on high surface area catalysts we saw no $m/z = 29$ amu that would indicate partial oxidation products, in support of our theoretical simulations. There was also no peak in the $m/z = 32$ amu trace indicating that all the p(4x4) structure has reacted with ethylene. This observation also rules out the possibility that CO_3^{2-} was present, as it would have desorbed as CO_2 and O_2. The desorption of the oxygen from the p(4x4) structure would occur at about 580 K [62].

The O 1s and C 1s spectra recorded after TPR (fig. 6c) show that the O 1s peak at 528 eV assigned to the oxygen on the reconstructed surface vanished completely and the peaks associated with H_xCO_2 and NO/NO_2 have shrunk substantially. Thus, from these experiments it appears that the oxygen in the p(4x4) reconstruction is only active in total oxidation. We also performed TPR experiments with higher C_2H_4 dosing (0.1 mbar ethylene for 10 min), which show similar results, although in this case there is an increase in the amount of $m/z = 44$ amu desorbing at 475 K, which is consistent with the expected higher initial coverage of AcH (see SI).

Conclusions

In summary, we have performed DFT calculations of the reaction of ethylene with oxygen in two well-known surface reconstructions, the p(2x1) structure on the Ag(110) and the p(4x4) structure on the Ag(111) surfaces. In both cases the calculations predict oxidation can occur through an OMC intermediate that decomposes into acetaldehyde, which is quickly converted to CO_2 on an oxygen-covered silver surface. And though we predict the dynamic nature of the p(4x4) reconstruction makes it active in room temperature ethylene oxidation, these dynamics alone are not enough to make the surface selective towards ethylene oxide production. TPR experiments of ethylene adsorbed on the oxygen-induced p(4x4) reconstruction on the Ag(111) surface confirm these predictions, with ethylene reacting at room temperature to form an adsorbed intermediate that desorbs as CO_2 upon heating. Thus, we have demonstrated that, alone, the oxygen-reconstructed silver surfaces that are thermodynamically favored under the oxygen chemical potentials required for ethylene epoxidation cannot produce the epoxide. These findings allow us to shift our focus away from these well-known structures and on to identifying new species and their roles in epoxidation.

Corresponding Author

*Email: trjones@fhi-berlin.mpg.de

Supporting Information

TPR results from high pressure experiments, structures of possible reaction intermediates, convergence tests for calculations, computed results with van der Waals (vdW) corrections.

References

1) van Santen, R. A.; de Groot, C.P.M. The Mechanism of Ethylene Epoxidation. *J. Catal.* **1986**, *98*, 530-539.

2) van Santen, R. A.; Kuipers, H. P. C. E. The Mechanism of Ethylene Epoxidation, In: *Advances in Catalysis*, D.D. Eley, Herman Pines, Paul B. Weisz, Editors, Academic Press **1987**, *35*, pp. 265-321.

3) Sachtler, W. M. H.; Backx, C.; van Santen, R. A. On the Mechanism of Ethylene Epoxidation. *Catal. Rev.* **1981**, *23*, 127-149.

4) Serafin, J. G.; Liu, A. C.; Seyedmonir, S. R. Surface Science and the Silver-Catalyzed Epoxidation of Ethylene: An Industrial Perspective. *J. of Mol. Catal. A: Chem.* **1998**, *131*, 157-168.

5) Bukhtiyarov, V. I.; Knop-Gericke, A. Ethylene Epoxidation over Silver Catalysts, In: *Nanostructured Catalysts: Selective Oxidations*, C. Hess, R. Schlögl, Editors, Cambridge: Royal Society of Chemistry **2011**, pp. 214-247.

6) Stegelmann, C.; Schiødt, N. C.; Campbell, C. T.; Stoltze, P. Microkinetic Modeling of Ethylene Oxidation over Silver. *J. Catal*. **2004**, *221*, 630–649.

7) Özbek, M. O.; Onal I.; Van Santen, R. A.; Ethylene epoxidation catalyzed by chlorine-promoted silver oxide. *J. Phys.: Condens. Matter* **2011**, *23*, 404202.

8) Özbek, M. O.; Van Santen, R. A.; The Mechanism of Ethylene Epoxidation Catalysis. *Catal. Lett*. **2013**, *143*, 131-141.

9) Li, W.-X.; Stampfl, C.; Scheffler, M. Insights into the Function of Silver as an Oxidation Catalyst by ab initio Atomistic Thermodynamics. *Phys. Rev. B* **2003**, *68*, 165412.

10) Reichelt, R.; Günther, S.; Rößler, M.; Wintterlin, J.; Kubias, B.; Jakobib, B.; Schlögl, R. High-pressure STM of the Interaction of Oxygen with Ag(111). *Phys. Chem. Chem. Phys*. **2007**, *9*, 3590-3599.

11) Bocquet, M.-L.; Sautet, P.; Cerda, J.; Carlisle, C. I.; Webb, M. J.; King, D. A. Specific Ethene Surface Activation on Silver Oxide Covered Ag{111} from the Interplay of STM Experiment and Theory. *J. Am. Chem. Soc*. **2003**, *125*, 3119-3125.

12) Bukhtiyarov, V. I.; Nizovskii, A. I.; Bluhm, H.; Hävecker, M.; Kleimenov, E.; Knop-Gericke, A.; Schlögl, R. Combined in situ XPS and PTRMS Study of Ethylene Epoxidation over Silver. *J. Catal*. **2006**, *238*, 260–269.

13) Rocha, T. C. R.; Oestereich, A.; Demidov, D. V.; Hävecker, M.; Zafeiratos, S.; Weinberg, G.; Bukhtiyarov, V. I.; Knop-Gericke, A.; Schlögl, R. The Silver–Oxygen System in Catalysis: New Insights by Near Ambient Pressure X-ray Photoelectron Spectroscopy. *Phys. Chem. Chem. Phys.* **2012**, *14*, 4554–4564.

14) Rocha, T. C. R.; Hävecker, M.; Knop-Gericke, A.; Schlögl, R. Promoters in Heterogeneous Catalysis: The Role of Cl on Ethylene Epoxidation over Ag. *J. Catal.* **2014**, *312*, 12-16.

15) Jones, T. E.; Rocha, T. C. R.; Knop-Gericke, A.; Stampfl, C.; Schlögl, R.; Piccinin, S. Thermodynamic and Spectroscopic Properties of Oxygen on Silver under an Oxygen Atmosphere. *Phys. Chem. Chem. Phys.* **2015**, *17*, 9288-9312.

16) Schmid, M.; Reicho, A.; Stierle, A.; Costina, I.; Klikovits, J.; Kostelnik, P.; Dubay, O.; Kresse, G.; Gustafson, J.; Lundgren, E.; *et al.* Structure of Ag(111)–*p*(4×4)–O: No Silver Oxide. *Phys. Rev. Lett.* **2006**, *96*, 146102.

17) Schnadt, J.; Michaelides, A.; Knudsen, J.; Vang, R. T.; Reuter, K.; Lægsgaard, E.; Scheffler, M.; Besenbacher, F. Revisiting the Structure of the *p*(4×4) Surface Oxide on Ag(111). *Phys. Rev. Lett.* **2006**, *96*, 146101.

18) Reichelt, R.; Günther, S.; Wintterlin, J.; Moritz, W.; Aballe, L.; Mentes, T. O. Low Energy Electron Diffraction and Low Energy Electron Microscopy Microspot *I/V* Analysis of the (4x4)O structure on Ag(111): Surface Oxide or Reconstruction? *J. Chem. Phys.* **2007**, *127*, 134706.

19) Schnadt, J.; Knudsen, J.; Hu, X. L.; Michaelides, A.; Vang, R. T.; Reuter, K.; Li, Z.; Lægsgaard, E.; Scheffler, M.; Besenbacher, F. Experimental and Theoretical Study of Oxygen Adsorption Structures on Ag(111). *Phys. Rev. B*, **2009**, *80*, 075424.

20) Bukhtiyarov, V. I.; Boronin, A. I.; Prosvirin, I. P.; Savchenko, V. I. Stages in the Modification of a Silver Surface for Catalysis of the Partial Oxidation of Ethylene: II. Action of the Reaction Medium. *J. Catal.* **1994**, *150*, 268-273.

21) Campbell, C. T.; Paffett, M. T. Model Studies of Ethylene Epoxidation Catalyzed by the Ag(110) Surface. *Surf. Sci.* **1984**, *139*, 396-416.

22) Bocquet, M.-L.; Michaelides, A.; Loffreda, D.; Sautet, P.; Alavi, A.; King, D. A. New Insights into Ethene Epoxidation on Two Oxidized Ag{111} Surfaces. *J. Am. Chem. Soc.* **2003**, *125*, 5620-5621.

23) Couves, J.; Atkins, M.; Hague, M.; Sakakini, B. H.; Waugh, K. C. The Activity and Selectivity of Oxygen Atoms Adsorbed on a Ag/α-Al$_2$O$_3$ Catalyst in Ethene Epoxidation. *Catal. Lett.* **2005**, *99*, 45-53.

24) Carlisle, C. I.; Fujimoto, T.; Sim, W. S.; King, D. A. Atomic Imaging of the Transition between Oxygen Chemisorption and Oxide Film Growth on Ag{111}. *Surf. Sci.*, **2000**, *470*, 15-31.

25) Günther, S.; Böcklein, S.; Wintterlin, J.; Niño, M. A.; Menteş, T. O.; Locatelli, A. Locating Catalytically Active Oxygen on Ag(1 1 1)—A Spectromicroscopy Study. *ChemCatChem* **2013**, *5*, 3342-3350.

26) Günther, S.; Menteş, T. O.; Niño, M. A.; Locatelli, A. Böcklein, S.; Wintterlin, J. Desorption Kinetics from a Surface Derived from Direct Imaging of the Adsorbate Layer. *Nature Comm.* **2014**, *5*, 3853.

27) Cant, N. W.; Hall, W. K. Catalytic Oxidation: VI. Oxidation of Labeled Olefins over Silver. *J. Catal.* **1978**, *52*, 81-94.

28) Linic, S.; Barteau, M. A. Formation of a Stable Surface Oxametallacycle that Produces Ethylene Oxide. *J. Am. Chem. Soc.* **2002**, *124*, 310-317.

29) Linic, S.; Barteau, M. A. Control of Ethylene Epoxidation Selectivity by Surface Oxametallacycles. *J. Am. Chem. Soc.* **2003**, *125*, 4034-4035.

30) Christopher, P.; Linic, S. Engineering Selectivity in Heterogeneous Catalysis: Ag Nanowires as Selective Ethylene Epoxidation Catalysts. *J. Am. Chem. Soc.* **2008**, *130*, 11264–11265.

31) Kokalj, A.; Gava, P.; de Gironcoli, S.; Baroni, S. What Determines the Catalyst's Selectivity in the Ethylene Epoxidation Reaction. *J. Catal.* **2008**, *254*, 304–309.

32) Greeley, J.; Mavrikakis, M. On the Role of Subsurface Oxygen and Ethylenedioxy in Ethylene Epoxidation on Silver. *J. Phys. Chem. C* **2007**, *111,* 7992-7999.

33) Ozbek M. O.; Onal, I.; van Santen, R. A. Effect of Surface and Oxygen Coverage on Ethylene Epoxidation. *Top. Catal.* **2012**, *55*, 710–717.

34) Twigg, G. H. The Mechanism of the Catalytic Oxidation of Ethylene. I. Experiments Using a Flow System. *Proc. Roy. Soc. London A: Math., Phys. and Eng. Sci.* **1946**, *188*, 92-104.

35) Kenson, R. E.; Lapkin, M. Kinetics and mechanism of ethylene oxidation. Reactions of ethylene and ethylene oxide on a silver catalyst. *J. Phys. Chem.* **1970**, *74*, 1493-1502.

36) Jones, T. E.; Rocha, T. C. R.; Knop-Gericke, A.; Stampfl, C.; Schlögl, R.; Piccinin, S. Insights into the Electronic Structure of the Oxygen Species Active in Alkene Epoxidation on Silver. *ACS Catal.* **2015**, *5*, 5846–5850.

37) Giannozzi, P.; Baroni, S.; Bonini, N.; Calandra, M.; Car, R.; Cavazzoni, C.; Ceresoli, D.; Chiarotti, G. L.; Cococcioni, M.; Dabo, I.; *et al*. QUANTUM ESPRESSO: A Modular and Open-Source Software Project for Quantum Simulations of Materials. *J. Phys.: Condens. Matter* **2009**, *21*, 395502.

38) Perdew, J. P.; Burke, K.; Ernzerhof, M. Generalized Gradient Approximation Made Simple. *Phys. Rev. Lett.* **1997**, *78*, 1396-1396.

39) Dal Corso, A. Pseudopotentials periodic table: From H to Pu. *Comput. Mater. Sci.* **2014**, *95*, 337-350.

40) Marzari, N.; Vanderbilt, D.; De Vita A.; Payne, M. C. Thermal Contraction and Disordering of the Al(110) Surface. *Phys. Rev. Lett.* **1999**, *82*, 3296-3299.

41) Grimme, S. Semiempirical GGA-type Density Functional Constructed with a Long-Range Dispersion Correction. *J. Comp. Chem.* **2006**, *27*, 1787-1799.

42) Becke, A. D.; Johnson, E. R. A Unified Density-Functional Treatment of Dynamical, Nondynamical, and Dispersion Correlations. II. Thermochemical and Kinetic Benchmarks. *J. Chem. Phys.* **2007**, *127*, 124108.

43) Otero-de-la-Roza, A.; Johnson, E. R. Van der Waals Interactions in Solids using the Exchange-Hole Dipole Moment Model. *J. Chem. Phys.* **2012**, *136*, 174109.

44) Pehlke, E.; Scheffler, M. Evidence for Site-Sensitive Screening of Core Holes at the Si and Ge (001) Surface. *Phys. Rev. Lett.* **1993**, *71*, 2338-2341.

45) Kaushik, V. K. XPS Core Level Spectra and Auger Parameters for Some Silver Compounds, *J. Electron. Spectrosc. Relat. Phenom.* **1991**, *56*, 273-277.

46) Rößler, M.; Geng, P.; Wintterlin, J. A High-Pressure Scanning Tunneling Microscope for Studying Heterogeneous Catalysis. *Rev. Sci. Instrum.* **2005**, *76*, 023705.

47) Bare, S. R.; GriffithsK.; , Lennard, W. N.; Tang, H. T. Generation of Atomic Oxygen on Ag(111) and Ag(110) using NO2: a TPD, LEED, HREELS, XPS and NRA Study. *Surf. Sci.* **1995**, *342*, 185-198.

48) Campbell, C. T.; Paffett, M. T. The Interactions of O2, CO and CO2 with Ag(110). *Surf. Sci.* **1984**, *143*, 517-535.

49) Pascal, M.; Lamont, C.; Baumgärtel, P.; Terborg, R.; Hoeft, J.; Schaff, O.; Polcik, M.; Bradshaw, A.; Toomes, R.; Woodruff, D. Photoelectron Diffraction Study of the Ag(110)-(2×1)-O Reconstruction. *Surf. Sci.* **2000**, *464*, 83-90.

50) Yang, L.; Rahman, T. S.; Bracco, G.; Tatarek, R. Missing-Row Reconstruction of Ag(110) Induced by a p(2×1) Oxygen Overlayer. *Phys. Rev. B* **1989**, *40*, 12271–12279.

51) Zambelli, T.; Barth, J. V.; Wintterlin, J. Formation Mechanism of the O-induced Added-Row Reconstruction on Ag(110): A Low-Temperature STM Study. *Phys. Rev. B* **1998**, *58*, 12663-12666.

52) Solomon, J. L.; Madix, R. J.; Stöhr, J. Orientation of Ethylene and Propylene on Ag(110) from Near Edge X-ray Adsorption Fine Structure. *J. Chem. Phys.* **1990**, *93*, 8379-8382.

53) Bocquet, M. L.; Loffreda, D. Ethene Epoxidation Selectivity Inhibited by Twisted Oxametallacycle: A DFT Study on Ag Surface-Oxide. *J. Am. Chem. Soc.* **2005**, *127*, 17207-1725.

54) Barteau, M. A.; Bowker, M.; Madix, R. J. Formation and Decomposition of Acetate Intermediates on the Ag(110) Surface. *J. Catal.* **1981**, *67*, 118-128.

55) Sault, A. G.; Madix, R. J. The Mechanism of Acetate Oxidation on Ag(110). *Surf. Sci.* **1986**, *172*, 598-614.

56) Grönbeck, H.; Klacar, S.; Martin, N. M.; Hellman, A.; Lundgren, E.; Andersen, J. N. Mechanism for Reversed Photoemission Core-Level Shifts of Oxidized Ag. *Phys. Rev. B* **2012**, *85*, 115445.

57) Sim, W. S.; Gardner, P.; King, D. A. Surface-Bound Helical Polyacetaldehyde Chains and Bidentate Acetate Intermediates on Ag{111} *J. Am. Chem. Soc.* **1996**, *118*, 9953-9959.

58) Sim, W. S.; Gardner, P.; King, D. A. Multiple Bonding Configurations of Adsorbed Formate on Ag{111}. *J. Phys. Chem.* **1996**, *100*, 12509-12516.

59) Polzonetti, G.; Alnot, P.; Brundle, C. R. The Adsorption and Reactions of NO2 on the Ag(111) Surface: I. XPS/UPS and Annealing Studies between 90 and 300 K. *Surf. Sci.* **1990**, *238*, 226-236.

60) Yeh, J. J.; Lindau, I. Atomic subshell photoionization cross sections and asymmetry parameters: $1 \leqslant Z \leqslant 103$. *At. Data. Nucl. Data Tables* **1985**, *32*, Pages 1-155.

61) Böcklein, S.; Günther, S.; Reichelt, R.; Wyrwich, R.; Joas, M.; Hettstedt, C.; Ehrensperger, M.; Sicklinger, J.; Wintterlin, J. Detection and Quantification of Steady-State Ethylene Oxide Formation over an Ag(111) Single Crystal. *J. Catal.* **2013**, *299*, 129-136.

62) Campbell, C. T. Atomic and molecular oxygen adsorption on Ag(111). *Surf. Sci.* **1985**, *157*, 43-60.